A&A 463, 703–706 (2007)
DOI: 10.1051/0004-6361:20066538

Astronomy & Astrophysics

On the nature of the cool component of MWC 560⋆

M. Gromadzki[1], J. Mikołajewska[1], P. A. Whitelock[2,3], and F. Marang[2]

[1] N. Copernicus Astronomical Center, Bartycka 18, 00-716 Warsaw, Poland
e-mail: marg@camk.edu.pl
[2] South African Astronomical Observatory, PO Box 9, Observatory, 7935, South Africa
[3] National Astrophysics and Space Science Programme, Department of Mathematics and Applied Mathematics, and the Department of Astronomy, University of Cape Town, South Africa

Received 10 October 2006 / Accepted 19 November 2006

ABSTRACT

Context. MWC 560 (V694 Mon) is one of the most enigmatic symbiotic system with a very active accretion-powered hot component. Such activity can be supported only by a luminous asymptotic giant branch star, i.e. a Mira or SR variable, with a high mass-loss rate. It is also a very unusual jet source because the jet axis lies practically parallel to the line of sight.
Aims. The aims of our study are the determination of the evolutionary status of the cool component of MWC 560.
Methods. Our methods involve analysis of near-IR $JHKL$ and optical light curves.
Results. The cool component of MWC 560 pulsates with a period of ∼340 days, and it is probably a red SR variable on the thermally pulsing AGB. The high mass-loss rate expected for such a star is sufficient to power the observed activity of the hot companion.

Key words. stars: binaries: symbiotic – stars: oscillations – stars: late-type – stars: mass-loss – stars: individual: MWC 560 (V694 Mon) – infrared: stars

1. Introduction

Discovered by Merrill & Burwell (1943) as a star with strong emission lines, MWC 560 (V694 Mon) is an enigmatic symbiotic system with a very active hot component. Its optical spectrum is always characterized by highly variable absorption features, blue-shifted by 1000–6000 km s^{-1}. These originate from H I, He I, Ca II and Fe II, and are detached from the stationary, narrow emission lines. The blue-shifted absorption features can be explained by a jet outflow along the line of sight (Tomov et al. 1990). In 1990, MWC 560 underwent a 2 mag photometric outburst, accompanied by spectacular changes in these blue shifted absorption lines (e.g. Tomov et al. 1990; Schmid et al. 2001, and references therein). The hot component is also a permanent source of rapid flickering with amplitudes in the range 0.2–0.7 mag on time scales of 10–100 min (e.g. Gromadzki et al. 2006, and references therein).

Both the flickering and the 1990 outburst characteristics suggest that the hot component is predominantly powered by unstable accretion, and its luminosity ∼100–1000 $L_\odot$ (Tomov et al. 1996; Mikołajewski et al. 1998) requires relatively high accretion rates of $\dot{M} \gtrsim 10^{-7} M_\odot \mathrm{yr}^{-1}$ (Schmid et al. 2001).

Doroshenko et al. (1993) found a 1930-day period in the $m_{\rm ph}$ historical light curve (Luthardt 1991) combined with more recent B-band photometry. They suggested an orbital origin of this period: if the orbit is eccentric, near periastron the accretion rate increases, and the hot component gets brighter.

We know rather little about the cool component of MWC 560. However, the high activity of its companion requires a high mass-loss rate, consistent with an evolved AGB star rather than a normal red giant. Absorption features in the optical spectrum suggest an M3−M4 spectral type (Sanduleak & Stephenson 1973; Allen 1978). Infrared spectral classification mainly based on TiO bands, and the CaII triplet indicates an M4−M5 giant (Szkody et al. 1990; Bopp 1990; Thakar & Wing 1992). Based on the lack of VO bands at 1.05 μm Meier et al. (1996) classified the cool component as an M5−M6 III giant. The most recent classification based on five TiO bands in the near infrared resulted in M5.5 and M6 (two different observations) (Mürset & Schmid 1999). Frąckowiak et al. (2003) found possible pulsations of red giant with P = 161 days, and concluded that it is an AGB star.

This paper contains an analysis of near infrared ($JHKL$) and visual (AAVSO and ASAS) light curves with the objective of searching for periodic changes and establishing the nature of the cool giant.

2. Observations

$JHKL$ broad-band photometry (1.25, 1.65, 2.2, 3.45 μm) was obtained with the MkII infrared photometer on the 0.75 cm telescope at SAAO, Sutherland (see Carter 1990 for details about the system). The measurements are good to ±0.03 at JHK and ±0.05 at L. The optical light curve consists of visual magnitude estimates collected by the American Association of Variable Stars Observers (AAVSO), and V-band photometry obtained in the frame of All Sky Automated Survey (ASAS) (Pojmański 2002). The near-IR observations cover the period from November 1984 to February 2004 (92 points in J and K bands, 91 in H and 86 in L) whereas the optical photometry was collected between April 1990 and December 2001 - the AAVSO data (2051 points), and from November 2000 to February 2006 - the ASAS data (330 points), respectively. The near-IR data are listed in Table 1 and the light curves are presented in Fig. 1.

⋆ Table 1 is only available in electronic form at http://www.aanda.org

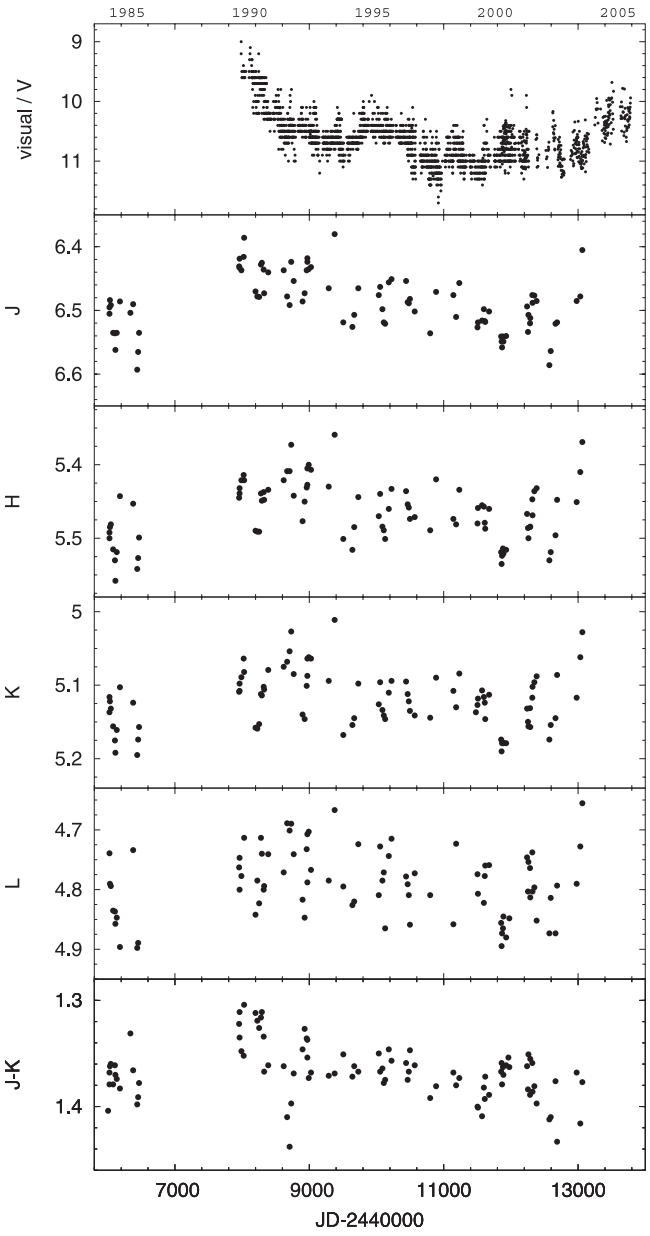

Fig. 1. Light curves for MWC 560. From *top* to *bottom*: AAVSO+ASAS and $JHKL$ light curves, and $J-K$ colours, respectively.

3. Period analysis

We analysed the near-IR, ASAS, and combined AAVSO+ASAS magnitudes by means of the program PERIOD[1] ver. 5.0, which uses the modified Lomb-Scargle method (Press & Rybicki 1989). To remove long-term trends from the optical data, a second order polynomial was subtracted from the combined AAVSO+ASAS light curve, and a third order spline function was subtracted from the ASAS light curve. The resulting power spectra are shown in the right panel of Fig. 2, and results of our period analysis are summarized in Table 2. The periods given in the table were derived from the maxima of the peaks in the periodograms ($f_{\max}^{-1}$), whereas their accuracy was estimated by calculating the half-size of a single frequency bin (Δf), centred on the peak (f_c) in a periodogram, and then converted to period units ($\Delta P = f_c^{-2} \cdot \Delta f$).

[1] Source of program is available on http://www.starlink.rl.ac.uk/

Power spectra of the composite AAVSO+ASAS light curve (Fig. 2, the uppermost, right panel) show a very pronounced peak at $1931^{\rm d}$ ($P_{\rm act}$) very close to the period reported by Doroshenko et al. (1993). The second and third harmonics, ~1931/2 and ~1931/3, respectively, are also present. We attribute this periodicity to repeated episodes of enhanced activity of the hot component following the ephemeris:

$$\mathrm{JD(max)} = 2\,448\,080 + 1931 \times E.$$

The light curve folded with this period is also show in Fig. 2 (the uppermost, left panel).

Power spectra corresponding to the $JHKL$ light curves are very similar to each other (Fig. 2). In all spectra the strongest peak corresponds to a 339-day period ($P_{\rm pul}$) which we take to be a real periodicity produced by pulsations of the cool component. There are also peaks around ~4500–5500 days (which is comparable to the time interval spanned by the data) connected with the long-term trend. Power spectra of the HK light curves show also peaks at $\sim 1900^{\rm d}$ days and $\sim 310^{\rm d}$. The former is very close to $P_{\rm act}$ found in the optical light curve whereas the latter seems to be an annual alias of 1900-day peak rather than a real periodicity. In the power spectrum of the J light curve the ~1900-day and ~310-day periods are not seen because they are overwhelmed by the strong long term trend. These periods are absent in the power spectrum of the L light curve. The following ephemeris gives the phases of maxima in the $JHKL$ bands:

$$\mathrm{JD(max)} = 2\,445\,960 + 339 \times E$$

and the light curves folded with this ephemeris are shown in Fig. 2 (left panel).

The power spectra of the visual photometry also show peaks at $\sim 310^{\rm d}$. These power spectra have poorer resolution that those for the near-IR data, so the peaks, especially that for the ASAS data, are relatively broad, and they may in fact be due to the $339^{\rm d}$ pulsation period combined with one year alias of the $1931^{\rm d}$ period. Such an interpretation is supported by the presence in the ASAS power spectrum of another peak at $\sim 166^{\rm d}$. This peak can be more accurately determined and it is due to the second harmonic of the pulsation period, which in this case would be $332^{\rm d}$. The ASAS light curve folded with this period is also shown in Fig. 2.

In the power spectrum of the AAVSO+ASAS data there is also a strong peak at $747^{\rm d}$ connected with a quasi-periodic oscillation which is predominantly visible during JD 2 450 500–2 452 300 (1997–2002). However, we note that it is very close to 2 years, and it may be an artifact.

4. Discussion and conclusions

Our near-IR photometry began in 1984, with only a dozen measurements over a 1.5-year interval. The observations restarted in 1990, when MWC 560 underwent an outburst, reaching the brightest level in its whole photometric history, and ejected jets (Tomov et al. 1990). In the near-IR, it brightened by ~0.1 mag in all, $JHKL$, bands. Then during the following 12 years, it slowly faded to the pre-outburst magnitudes observed in 1984. In 2002–2004, the star brightened again. The point scatter of the near-IR light curves was always of ~0.1 mag in JHK bands, and ~0.2 mag in L band, respectively. In general, the near-IR light curves reflect the trend shown by the visual/V light curve, with additional maxima around JD 2 450 000 and JD 2 452 000. The $J-K$ colour becomes redder as the brightness declines (Fig. 1) due to a decreasing contribution from the hot component.

Table 2. Peaks in power spectra.

Frequency days^{-1}	Period days	Power sigma unit	Remarks
J			
2.9479×10^{-3}	339 ± 4	20.8	$P_{\rm pul}$
H			
5.3276×10^{-4}	1877 ± 126	7.0	$P_{\rm act}$
2.9479×10^{-3}	339 ± 4	19.8	$P_{\rm pul}$
3.2321×10^{-3}	309 ± 3	10.6	alias
K			
5.3276×10^{-4}	1877 ± 126	7.2	$P_{\rm act}$
2.9479×10^{-3}	339 ± 4	20.2	$P_{\rm pul}$
3.2676×10^{-4}	306 ± 3	12.2	alias
L			
2.9487×10^{-3}	339 ± 4	11.6	$P_{\rm pul}$
ASAS			
3.2708×10^{-3}	306 ± 12	35.8	$P_{\rm ASAS}$
6.0183×10^{-3}	166 ± 4	18.5	$P_{\rm pul}/2$
AAVSO+ASAS			
5.1789×10^{-4}	1931 ± 162	285.6	$P_{\rm act}$
9.4946×10^{-4}	1053 ± 48	57.9	$P_{\rm act}/2$
1.3379×10^{-3}	747 ± 24	102.4	
3.1937×10^{-3}	313 ± 4	53.1	$P_{\rm ASAS}$, alias

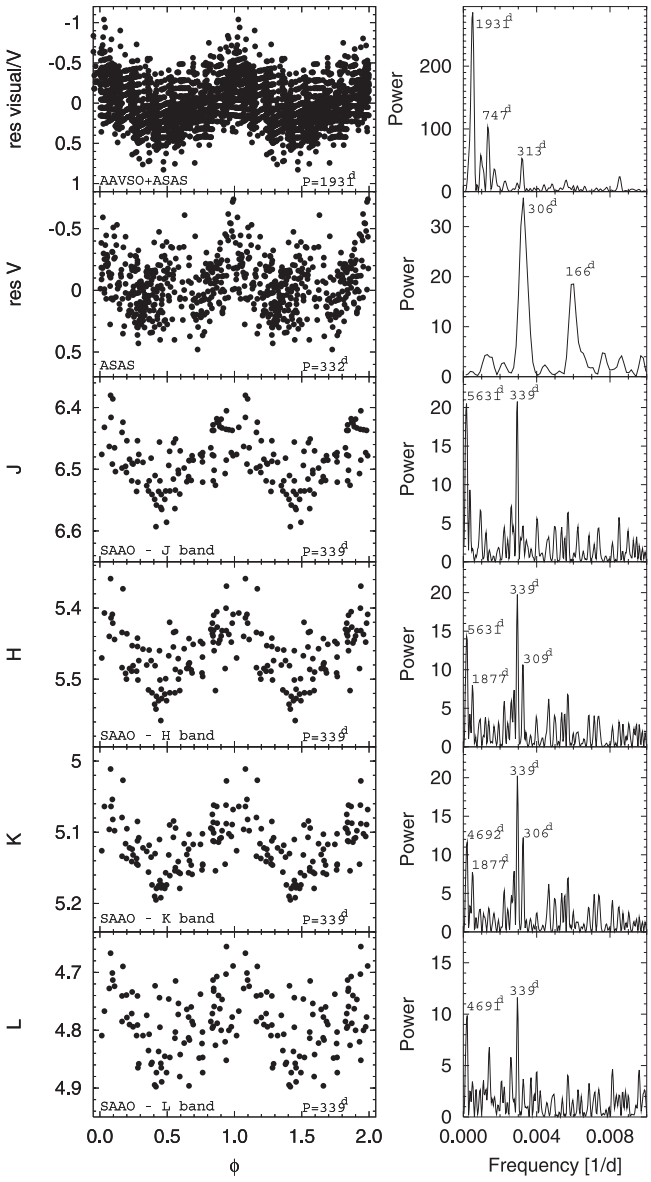

Fig. 2. Power spectra (*right*) and corresponding light curves folded with the strongest period (*left*). From the top to bottom: AAVSO+ASAS light curve folded with period $P_{\rm act}$ = 1931 days, ASAS light curve folded with period $P_{\rm ASAS}$ = 332 days, and *JHKL* light curves all folded with period $P_{\rm pul}$ = 339 days, respectively.

Our period analysis of the *JHKL* light curves revealed a 339-day periodicity which can be attributed to radial pulsations of the M giant. Although this period is close to that of Mira itself, and of many other Galactic Mira variables, the amplitude of the pulsation, $\Delta K \sim 0.1$ mag, is much lower than $\Delta K \gtrsim 0.4$ mag observed in Miras, including typical symbiotic Miras (Whitelock 1987). We therefore classify it as an SRa variable (using the definition in the GCVS4) rather than as a Mira. This pulsation is hardly detectable in the visual light because radiation in this range is dominated by the very active hot component. In fact, the scatter of points from the folded light curve in Fig. 2, $\Delta V \sim 0.3 \div 0.6$ mag is comparable to the amplitude of the flickering (Gromadzki et al. 2006) which complicates the period analysis. The red giant pulsation period found in this study is more than twice the 161-day pulsation period reported by Frąckowiak et al. (2003), and it is the only periodicity present in all bands.

The basic properties and evolutionary status of the semi-regular variables (SRVs) of type SRa and SRb were discussed in detail by Kerschbaum & Hron (1992, 1994, 1996). In particular, they found that the SRas appear as intermediate objects between Miras and SRbs in all aspects, including periods, amplitudes and mass-loss rates. They also concluded that the SRas do not form a distinct class of variables, but are a mixture of "intrinsic" Miras and SRbs. The SRbs split into a "blue" group with $P < 150$ days and no indication of circumstellar shells and a "red" group with temperatures and mass-loss rates comparable to Miras, but periods about half as long. They suggested that the "red" and "Mira" SRbs are thermally pulsing AGB-stars (Kerschbaum & Hron 1992). The persistent and relatively long period places the cool component of MWC 560 among the "Mira" SRVs. These differ from normal Miras only in their smaller pulsation amplitudes. The IRAS [12 μm]–[25 μm] = 0.64 locates MWC 560 in the period–IRAS colour diagram of (Kerschbaum & Hron 1992) in the region occupied by 86% of the Miras, whereas most SRbs are outside this region. The average, reddening corrected ($E_{B-V} = 0.15$; Schmid et al. 2001) near-IR colours $\langle H-K\rangle_0 = 0.30$, $\langle J-H\rangle_0 = 1.00$, $K - [12\,\mu{\rm m}] = 1.25$, and the spectral type M5.5–6 are also consistent with an O-rich SRV, although the colours are unlike those of a Mira. Finally, if the 1931 day periodicity is orbital then the two stars of this symbiotic system are close to each other (see below), and the presence of a nearby companion may influence the pulsation characteristics, possibly reducing the pulsation amplitude. We suggest that the evidence supports the view that the red component of MWC 560 is on the TP AGB-phase.

The SRV component of MWC 560 could be the source of a strong stellar wind and thus support the observed high activity of the hot component. If we estimate the mass of the red giant at 1 $M_\odot$ and that of the white dwarf companion at 0.5 $M_\odot$ then,

assuming that the 5.3 year period is orbital, the separation of the two stars will be 3.55 AU and the radius of the Roche lobe for the M giant in a circular orbit will be 1.5 AU. Schmid et al. (2001) argued that an accretion rate up to a few $\times 10^{-7}\,M_{\odot}\,\mathrm{yr}^{-1}$ is necessary to account for the observed hot component luminosity which is comparable to the wind efficiency found for typical Miras and SRVs. For example, Olofsson et al. (2002) determined average mass loss rate of $2 \times 10^{-7}\,M_{\odot}\,\mathrm{yr}^{-1}$, with a maximum value of $8 \times 10^{-7}\,M_{\odot}\,\mathrm{yr}^{-1}$ for a sample of M-type irregular and semi-regular variables. So, in the case of MWC 560, a significant fraction of the mass lost in the cool giant wind must be accreted by the hot companion. This is possible only if the binary components of MWC 560 interact via "wind Roche lobe" overflow occurs instead of a spherically symmetric wind (Podsiadlowski 2007).

One of the most intriguing features of this hot component activity is its highly periodic character. The 1931-day periodicity found in the visual AAVSO+ASAS light curve is essentially identical with the 1930-day periodicity detected in the m_{pg}/B light curve by Doroshenko et al. (1993). We note that this periodicity remained in-phase over a century, and the most natural explanation would be an orbital motion. The only problem with the orbital interpretation is that the orbital inclination of MWC 560 seems to be extremely low (as indicated by the jet axis practically aligned with the line of sight, and the lack of orbitally related radial velocity changes) which excludes any geometrical effects, such as eclipses, illumination, etc. Although one can argue that the jet axis can be inclined with respect to the binary orbital plane, the relatively large amplitude of this variability, $\Delta m_{\mathrm{pg}} \sim 1$ and $\Delta V \sim 0.5$ mag, respectively, points to another mechanism(s). One possibility is an eccentric orbit and enhanced accretion rate near periastron passage causing a brightening of the hot component (Doroshenko et al. 1993). Then we can even speculate that if the eccentricity is high enough, ∼0.5 or more, a Roche lobe overflow may occur near the periastron.

Another possibility is enhanced mass loss due to periodic changes in the SRV environment. We note that the 1931 day period equals roughly six times the pulsation period. A periodically enhanced mass loss might be caused by some kind of interplay between the cool component pulsation and layered dust formation shells. Such effects have been shown by time-dependent hydrodynamic simulation of C-rich Mira environmentsenvironment. We note that the 1931 day period equals roughly six times the (Winters et al. 1999; Winters & Le Bertre 2001). In particular, these simulations have been able to reproduce variations of the mass-loss rates on different time scales.

Acknowledgements. This study made use of the American Association of Variable Star Observers (AAVSO) International Database contributed by observers worldwide and the public domain database of The All Sky Automated Survey (ASAS) which we acknowledged. We also thank the following people for making IR observations: Greg Roberts, Robin Catchpole, Brian Carter, Dave Laney and Hartmut Winkler. This research was partly supported by KBN grant 1P03D 017 27.

References

Allen, D. A. 1978, MNRAS, 184, 601
Bopp, B. W. 1990, IAU Circ., 5151
Carter, B. S. 1990, MNRAS, 242, 1
Doroshenko, V. T., Goranskij, V. P., & Efimov, Y. S. 1993, IBVS, 3824
Frąckowiak, S. M., Mikołajewski, M., & Tomov, T. 2003, in Symbiotic Stars Probing Stellar Evolution, ed. R. L. M. Corradi, J. Mikołajewska, & T. J. Mahoney, ASP Conf. Ser., 303, 120
Gromadzki, M., Mikołajewski, M., Tomov, T., et al. 2006, Acta Astron., 56, 97
Kerschbaum, F., & Hron, J. 1992, A&A, 263, 97
Kerschbaum, F., & Hron, J. 1994, A&AS, 106, 397
Kerschbaum, F., & Hron, J. 1996, A&A, 308, 489
Luthardt, R. 1991, IBVS, 3563
Meier, S. R., Rudy, R. J., Lynch, D. K., et al. 1996, AJ, 111, 476
Merrill, P. W., & Burwell, C. G. 1943, ApJ, 98, 153
Mikołajewski, M., Janowski, J. L., Tomov, T., et al. 1998, IBVS, 4598
Mürset, U., & Schmid, H. M. 1999, A&AS, 137, 473
Olofsson, H., González Delgado, D., Kerschbaum, F., & Schöier, F. L. 2002, A&A, 391, 1053
Podsiadlowski, P. 2007, in Evolution and chemistry of symbiotic stars, binary post-AGB and related objects, ed. J. Mikołajewska, & R. Szczerba, Baltic Astron., 16-1
Pojmański, G. 2002, Acta Astron., 52, 397
Press, W. H., & Rybicki, G. B. 1989, ApJ, 338, 277
Sanduleak, N., & Stephenson, C. B. 1973, ApJ, 185, 899
Schmid, H. M., Kaufer, A., Camenzind, M., et al. 2001, A&A, 377, 206
Szkody, P., Mateo, M., & Schmeer, P. 1990, IAU Circ., 4987
Thakar, A., & Wing, R. E. 1992, BAAS, 24, 801
Tomov, T., Kolev, D., Georgiev, L., et al. 1990, Nature, 346, 637
Tomov, T., Kolev, D., Ivanov, M., et al. 1996, A&AS, 116, 1
Whitelock, P. A. 1987, PASP, 99, 573
Winters, J. M., & Le Bertre, T. 2001, in Astrophysics and Space Science Library, Post-AGB Objects as a Phase of Stellar Evolution, ed. R. Szczerba, & S. K. Górny (Kluwer Academic Publishers), 265, 93
Winters, J. M., Le Bertre, T., & Keady, J. J. 1999, in Asymptotic Giant Branch Stars, ed. T. Le Bertre, A. Lebre, & C. Waelkens, IAU Symp., 191, 261

Online Material

Table 1. IR photometry of MWC 560.

JD –2 440 000 (day)	*J*	*H*	*K*	*L*
		(mag)		
6024.55	6.50	5.49	5.12	
6026.45	6.51	5.50	5.14	4.74
6034.53	6.48	5.49	5.12	4.79
6043.57	6.49	5.48	5.13	4.79
6082.46	6.54	5.52	5.16	4.84
6108.39	6.54	5.53	5.18	4.84
6113.33	6.56	5.56	5.19	4.86
6136.30	6.54	5.52	5.16	4.85
6184.24	6.49	5.44	5.10	4.90
6338.57	6.50			
6380.61	6.49	5.45	5.12	4.73
6440.46	6.59	5.54	5.20	4.90
6454.48	6.56	5.53	5.17	4.89
6465.35	6.54	5.50	5.16	
7958.39	6.43	5.45	5.11	4.76
7961.37	6.42	5.44	5.11	4.80
7964.33	6.43	5.43	5.10	4.75
7989.26	6.44	5.42	5.09	4.78
8023.22	6.42	5.41	5.06	
8028.19	6.39	5.42	5.08	4.71
8197.59	6.47	5.49	5.16	4.84
8227.56	6.48	5.49	5.16	4.79
8252.56	6.48	5.49	5.15	4.82
8280.49	6.43	5.44	5.11	4.71
8294.38	6.43	5.45	5.11	4.74
8320.40	6.44	5.44	5.10	4.80
8326.41	6.47	5.45	5.11	4.79
8390.20	6.44	5.43	5.08	4.74
8617.53	6.44	5.42	5.08	4.77
8670.41	6.48	5.41	5.07	4.69
8705.33	6.49	5.41	5.05	4.70
8731.29	6.42	5.37	5.03	4.69
8768.20	6.45	5.44	5.09	4.74
8899.63	6.49	5.48	5.14	4.82
8932.56	6.47	5.45	5.15	4.85
8960.52	6.44	5.43	5.10	4.73
8968.44	6.42	5.41	5.06	4.71
8969.52	6.42	5.43	5.09	4.79
8991.41	6.44	5.40	5.06	4.70
9024.42	6.43	5.41	5.06	4.77
9292.54	6.47	5.43	5.09	4.79
9379.36	6.38	5.36	5.01	4.67
9503.19	6.52	5.50	5.17	4.80
9643.62	6.53	5.52	5.15	4.83
9667.53	6.51	5.49	5.15	4.82
9728.50	6.47	5.44	5.10	4.72
10035.54	6.48	5.47	5.13	4.81
10053.60	6.46	5.44	5.10	4.73
10086.47	6.50	5.48	5.13	4.79
10110.42	6.52	5.49	5.14	4.77
10126.45	6.52	5.50	5.15	4.87
10181.29	6.46	5.46	5.11	4.74
10221.22	6.45	5.43	5.09	4.72
10437.54	6.45	5.44	5.10	4.78
10464.46	6.49	5.45	5.11	4.79
10478.37	6.49	5.46	5.12	4.81
10498.39	6.48	5.47	5.14	4.86

Table 1. continued.

JD –2 440 000 (day)	*J*	*H*	*K*	*L*
		(mag)		
10567.23	6.50	5.47	5.14	4.77
10801.51	6.54	5.49	5.14	4.81
10884.38	6.47	5.42	5.09	
11146.59	6.48	5.47	5.11	4.86
11187.48	6.51	5.48	5.13	4.72
11234.30	6.46	5.43	5.08	
11479.54			5.14	
11505.51	6.53	5.48	5.13	4.77
11511.48	6.52	5.46	5.12	4.81
11572.48	6.52	5.46	5.11	
11599.35	6.50	5.46	5.12	4.82
11611.33	6.52	5.48	5.12	4.78
11617.34	6.52	5.49	5.15	4.76
11675.24	6.50	5.46	5.11	4.76
11857.58	6.54	5.52	5.17	4.86
11864.58	6.55	5.54	5.19	4.90
11869.52	6.56	5.52	5.18	4.87
11881.54	6.54	5.51	5.18	4.87
11890.57	6.55	5.52	5.18	4.85
11927.47	6.54	5.52	5.18	4.88
11976.31				4.85
12239.58	6.49	5.47	5.13	4.75
12255.57	6.53	5.49	5.15	4.80
12263.47	6.51	5.50	5.16	4.75
12284.50	6.52	5.49	5.13	4.76
12289.44	6.51	5.48	5.16	4.81
12319.40	6.48	5.45	5.12	4.74
12324.44	6.49	5.47	5.10	4.80
12349.32	6.48	5.44	5.10	4.80
12384.26	6.49	5.43	5.09	4.85
12572.58	6.59	5.53	5.17	4.87
12594.60	6.56	5.52	5.15	4.81
12664.43	6.52	5.50	5.15	4.87
12690.38	6.52	5.45	5.09	4.79
12979.55	6.49	5.45	5.12	4.79
13031.48	6.48	5.41	5.06	4.73
13063.34	6.41	5.37	5.03	4.66